2328 © 1991 The Chemical Society of Japan Bull. Chem. Soc. Jpn., 64, 2328—2334 (1991) [Vol. 64, No. 8

Combustion Reactions in Silane–Air Flames
I. Flat Premixed Flames

Seishiro Fukutani,* Yasuhiro Uodome, Nílson Kunioshi, and Hiroshi Jinno†
Department of Industrial Chemistry, Faculty of Engineering, Kyoto University,
Yoshida-honmachi, Sakyo-ku, Kyoto 606
†Department of Chemistry, Faculty of Science and Engineering, Sophia University,
Kioicho 7-1, Chiyoda-ku, Tokyo 102
(Received April 1, 1991)

In this work the combustion mechanism of silane–air flames is elucidated through a simulation employing a detailed chemical scheme. Two different pathways for the consumption of silane were found: $SiH_4 \rightarrow SiH_3 \rightarrow SiH_2O \rightarrow HSiO$, which proceeds in low-temperature regions, and $SiH_4 \rightarrow SiH_2 \rightarrow HSiO$, occurring at high temperatures; this supports results previously reported in the literature. It was also found that some reactions occur over wide ranges of temperature and that the governing step for the whole silane combustion is the reaction of silane with hydroxyl radicals. A least square fitting to the burning velocities and adiabatic flame temperatures obtained for the four investigated mixtures, with equivalence ratios of 2.0, 1.43, 1.0, and 0.5, indicated that a mixture with equivalence ratio of about 1.2 would have the largest burning velocity and the highest flame temperature.

The oxidation of silicon tetrachloride or silane yields silicon dioxide in condensed states. The production of solid or liquid phases from gases is a complicated phenomenon comprising chemical reactions and physical processes such as nucleation and crystal growth; it is interesting and, at the same time, important to investigate these processes from standpoints of both fundamental and applied researches on production of clusters and fine particles or on the CVD methods.

Silane is widely used as a silicon-containing material in semiconductor industries, for instance. This species is, however, spontaneously explosive in the air or sometimes causes production of undesirable products because of its high reactivity. The reaction between silane and oxygen should be investigated in detail to treat them safely and to maintain their efficient reactions. This work aims to simulate flat premixed silane–air flames using a model which neglects the physical processes to avoid complexities, and to elucidate the mechanisms of silane–oxygen combustion reactions under various conditions.

Recently some experimental and theoretical works have been done on the chemistry of silane. McLain et al.[1,2] have proposed the most reliable reaction schemes at present for the combustion of silane, which has been derived on the basis of the similarity to that of methane, and compared the predicted ignition delay times with the corresponding experimental values. Koda et al.[3–7] have studied experimentally silane combustion reactions by use of counterflow diffusion flames, and Tokuhashi et al.[8] have experimentally and theoretically investigated premixed silane flames. The explosion behavior of silane–oxygen mixtures has been investigated by Hartman et al.[9] in thermochemical discussion on the reaction mechanism. In spite of these pioneering works, the mechanism of silane combustion is still left unknown in many points. At present it is inevitable to accumulate the information in this field by both experimental and theoretical approaches.

Simulation Model

We used the same assumptions as those made in a previous work[10] in constructing the simulation model. Additional assumptions applicable only for this investigation are that (1) silicon dioxide exists in condensed phases over the temperature range considered here: high-temperature cristobalite phase below 1996 K and liquid phase above it; (2) only chemical processes are considered in the formation of silicon dioxide and hence the processes of condensation or crystallization such as nucleation and crystal growth are neglected. According to these two assumptions the produced silicon dioxide is removed from the gaseous reaction system but its amount is evaluated in terms of molar concentration and not of the size or number of silica particles. As thermochemical data for silicon dioxide, the data for high-temperature cristobalite were used below 1996 K and those corresponding to the liquid state were employed above the melting point.

The governing equations are expressed as follows:

$$\frac{\partial \rho}{\partial t}+\frac{\partial}{\partial x}(\rho v)=0 \tag{1}$$

$$\frac{\partial}{\partial t}(c_p\rho T)+\frac{\partial}{\partial x}(c_p\rho Tv) =\frac{\partial}{\partial x}\left(\lambda\frac{\partial T}{\partial x}\right)+\sum_i D_i\rho\frac{\partial h_i}{\partial x}\frac{\partial \omega_i}{\partial x}-\sum_i h_i\varphi_i \tag{2}$$

$$\frac{\partial}{\partial t}(\rho\omega_i)+\frac{\partial}{\partial x}(\rho\omega_i v)=\frac{\partial}{\partial x}\left(D_i\rho\frac{\partial \omega_i}{\partial x}\right)+\varphi_i \tag{3}$$

$$p=\rho RT\sum_i\frac{\omega_i}{m_i} \tag{4}$$

where ω_i and φ_i are the mass fraction and chemical production rate of the i-th species. The other symbols have their usual meanings.

The partial differential terms were discretized into the corresponding finite difference terms according to the

Table 1. SiH_4-H_2-O_2 Reaction Scheme[a)]
$k=AT^n\exp(-E/T)$

No.	Reaction	A	n	E	Ref.
R1	$H_2+O_2 \longrightarrow OH+OH$	2.50E06	0.0	19630	12
R2	$H+O_2 \longrightarrow OH+O$	1.20E11	−0.91	8310	13
R3	$O+H_2 \longrightarrow OH+H$	1.50E01	2.0	3800	13
R4	$OH+OH \longrightarrow O+H_2O$	1.50E03	1.14	0	13
R5	$OH+H_2 \longrightarrow H+H_2O$	1.00E02	1.6	1660	13
R6	$H+H+M \longrightarrow H_2+M$	9.70E04	−0.6	0	13
R7	$O+O+M \longrightarrow O_2+M$	2.86E05	−1.0	0	13
R8	$H+O+M \longrightarrow OH+M$	3.60E06	−1.0	0	14
R9	$OH+H+M \longrightarrow H_2O+M$	2.15E10	−2.0	0	13
R10	$H+O_2+M \longrightarrow HO_2+M$	2.00E06	−0.8	0	13
R11	$H+HO_2 \longrightarrow H_2+O_2$	2.50E07	0.0	350	13
R12	$H+HO_2 \longrightarrow OH+OH$	1.50E08	0.0	500	13
R13	$H+HO_2 \longrightarrow O+H_2O$	5.00E07	0.0	500	12
R14	$OH+HO_2 \longrightarrow H_2O+O_2$	2.00E07	0.0	0	13
R15	$O+HO_2 \longrightarrow OH+O_2$	2.00E07	0.0	0	13
R16	$HO_2+H_2 \longrightarrow H+H_2O_2$	7.30E05	0.0	9390	13
R17	$HO_2+HO_2 \longrightarrow H_2O_2+O_2$	2.00E06	0.0	0	13
R18	$OH+H_2O_2 \longrightarrow HO_2+H_2O$	7.00E06	0.0	720	13
R19	$H+H_2O_2 \longrightarrow OH+H_2O$	1.00E07	0.0	1800	13
R20	$O+H_2O_2 \longrightarrow OH+HO_2$	2.80E07	0.0	3220	13
R21	$OH+OH+M \longrightarrow H_2O_2+M$	3.25E10	−2.0	0	13
R22	$SiH_4 \longrightarrow SiH_2+H_2$	3.30E12	0.0	25720	2
R23	$SiH_4+O_2 \longrightarrow SiH_3+HO_2$	2.00E05	0.0	22150	2
R24	$SiH_4+HO_2 \longrightarrow SiH_3+H_2O_2$	3.00E06	0.0	2820	2
R25	$SiH_4+H \longrightarrow SiH_3+H_2$	1.50E07	0.0	1260	2
R26	$SiH_4+O \longrightarrow SiH_3+OH$	4.20E06	0.0	810	2
R27	$SiH_4+OH \longrightarrow SiH_3+H_2O$	8.40E06	0.0	50	2
R28	$SiH_3+H \longrightarrow SiH_2+H_2$	1.50E07	0.0	1260	2
R29	$SiH_3+O \longrightarrow SiH_2O+H$	1.30E08	0.0	1010	2
R30	$SiH_3+OH \longrightarrow SiH_2O+H_2$	5.00E06	0.0	0	2
R31	$SiH_3+O_2 \longrightarrow SiH_2O+OH$	8.60E08	0.0	5750	2
R32	$SiH_2+O_2 \longrightarrow HSiO+OH$	1.00E08	0.0	1860	2
R33	$SiH_2O+M \longrightarrow HSiO+H+M$	5.00E10	0.0	38570	2
R34	$SiH_2O+H \longrightarrow HSiO+H_2$	3.30E08	0.0	5290	2
R35	$SiH_2O+O \longrightarrow HSiO+OH$	1.80E07	0.0	1550	2
R36	$SiH_2O+OH \longrightarrow HSiO+H_2O$	7.50E06	0.0	90	2
R37	$SiH_2O+HO_2 \longrightarrow HSiO+H_2O_2$	1.00E06	0.0	4030	2
R38	$HSiO+M \longrightarrow SiO+H+M$	5.00E08	0.0	14600	2
R39	$HSiO+H \longrightarrow SiO+H_2$	2.00E08	0.0	0	2
R40	$HSiO+O \longrightarrow SiO+OH$	1.00E08	0.0	0	2
R41	$HSiO+OH \longrightarrow SiO+H_2O$	1.00E08	0.0	0	2
R42	$HSiO+O_2 \longrightarrow SiO+HO_2$	1.20E08	0.0	2000	2
R43	$SiO+O+M \longrightarrow SiO_2+M$	2.50E03	0.0	2200	2
R44	$SiO+OH \longrightarrow SiO_2+H$	4.00E06	0.0	2870	2
R45	$SiO+O_2 \longrightarrow SiO_2+O$	1.00E07	0.0	3270	2

a) The rate constants are expressed in m, mol, s units.

control-volume method;[11)] the meshes have unequal sizes being roughly proportional to the product of the temperature and its gradient so that even fast reactions occurring there can be simulated with accuracy.

The boundary conditions at the unburned side are that the gas mixture is at 298 K and has given composition and velocity, and those at the burned side are that all the gradients of the dependent variables are zero.

A reaction scheme composed of forty-five pairs of elementary reactions was used for silane combustion; the first twenty-one pairs of reactions belong to hydrogen combustion, and the rest are reactions of silicon-containing species, which are SiH_4, SiH_3, SiH_2, SiH_2O, HSiO, SiO, and SiO_2, and were selected from the most reliable scheme at present (Table 1).

Since produced silicon dioxide is extinguished from the system the reverse reactions of (R43), (R44), and (R45) are neglected; in the actual system, however, the chemical equilibrium is reached between the gaseous and the condensed phases of silicon dioxide at high temperatures, and these reactions have their reverse partners.

Results and Discussion

Stoichiometric Flame. Figure 1 shows the profiles of the temperature and the stable species mole fractions in a stoichiometric silane-air premixed flame and Figs. 2 and 3 show those of active species. The abscissas of these figures are, strictly speaking, the distance from an arbitrary origin. As described above, silicon dioxide is not a gaseous component, but, for convenience' sake, it is referred to with the mole fraction defined as the quotient of its concentration over the total concentration of the gaseous phase.

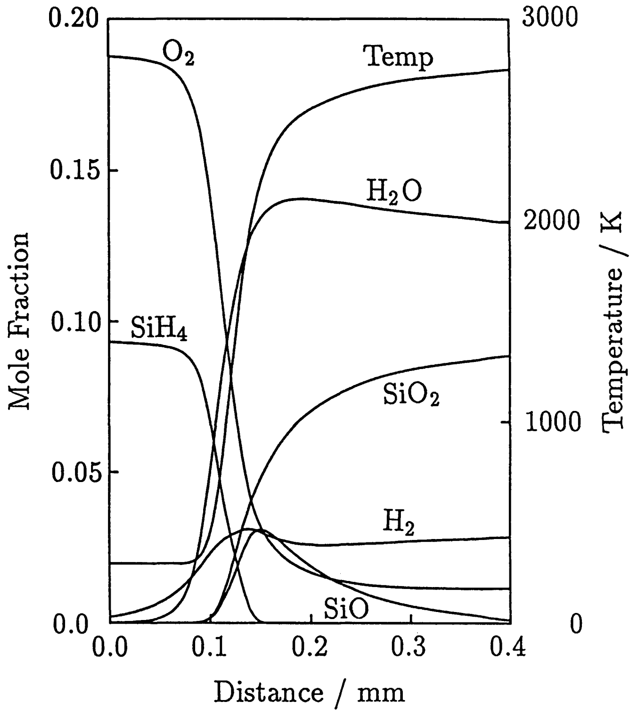

Fig. 1. Profiles of the temperature and the concentrations of stable species in the stoichiometric silane flame.

The reaction zone is about 0.05 mm thick and very thin in comparison with those of hydrogen and methane premixed flames; the combustion reaction is confined within this thin area. The second last and the last oxidation products of silane, that is, SiO and SiO_2, appear at fairly high temperatures, but hydrogen and water are present even at room temperature; their presence at low temperatures suggests that these species are produced at an early stage of silane combustion though hydrogen, in particular, has a large diffusion coefficient and diffuses from the high-temperature region to extremely upstream zones.

The intermediate species of silane combustion reactions, SiH_3, SiH_2, SiH_2O, and HSiO, are not distributed in a common region; SiH_3 appears in a low-temperature region, both SiH_2 and HSiO in a high-temperature region, and SiH_2O over a wide temperature range.

The three active species of the hydrogen-oxygen system, OH radicals and H and O atoms, increase above 1000 K. Hydroxyl radicals are particularly present in a large amount even in the low-temperature region comparing with that in hydrogen premixed flames.10) Hydroperoxyl radicals are scattered widely and clearly have a shoulder in their profile suggesting that different reaction mechanisms contribute to their production depending on temperature.

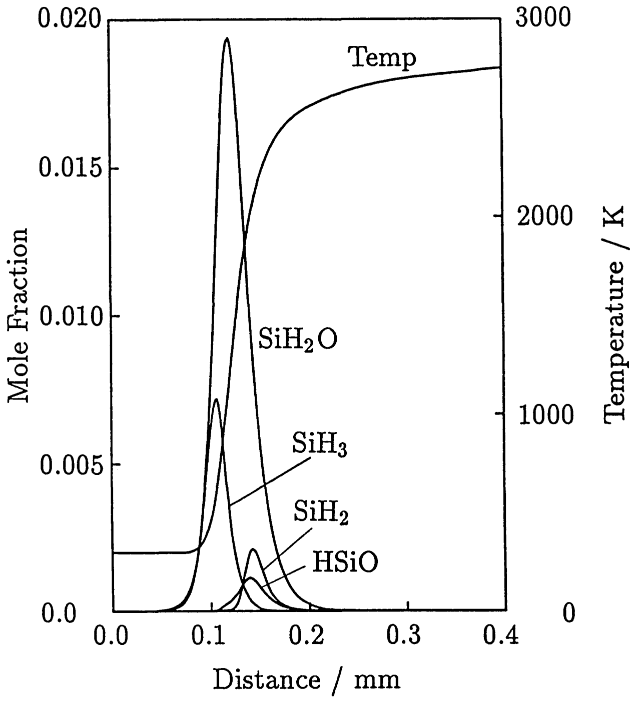

Fig. 2. Profiles of the temperature and the concentrations of intermediate silicon-containing species in the stoichiometric silane flame.

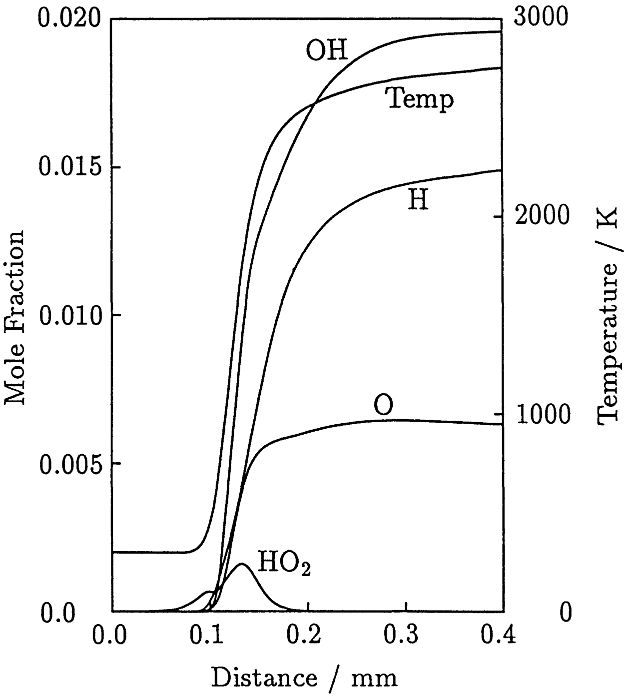

Fig. 3. Profiles of the temperature and the concentrations of intermediate hydrogen-oxygen-containing species in the stoichiometric silane flame.

Koda et al.[7] has already pointed out that the reaction scheme proposed by McLain gives two alternative pathways in the silane reaction from SiH_4 to HSiO: one via SiH_3 and the other via SiH_2. Our simulation also supports their result.

Figures 4 and 5 show, respectively, the reaction rates and the heat release rates for the predominant silicon-containing species reactions as functions of temperature. The profiles indicate that those reactions can be classified into three different groups based on the temperature range of their activation: low-temperature reactions, high-temperature reactions and wide-temperature-range reactions.

Reactions

$$SiH_4 + OH \rightarrow SiH_3 + H_2O, \qquad (R27)$$

$$SiH_4 + H \rightarrow SiH_3 + H_2, \qquad (R25)$$

$$SiH_3 + O_2 \rightarrow SiH_2O + OH, \qquad (R31)$$

$$SiH_3 + O \rightarrow SiH_2O + H, \qquad (R29)$$

and

$$SiH_2O + OH \rightarrow HSiO + H_2O \qquad (R36)$$

are low-temperature reactions. They oxidize silane following the sequence $SiH_4 \rightarrow SiH_3 \rightarrow SiH_2O \rightarrow HSiO$. Hydroxyl radicals hold a particularly important role at the first step of this series of reactions due to their cyclic consumption and production by reactions (R27) and (R31). Since reaction (R27) is already activated and also begins to release considerable amounts of heat at temperatures as low as 500 K, it can be considered the most important of the governing elementary steps for the low-temperature combustion mechanism. At temperatures higher than 700 K, SiH_3 is oxidized by oxygen to SiH_2O through reaction (R31) with formation of hydroxyl radicals, and the SiH_2O is dehydrogenated with hydroxyl radicals by reaction (R36); reactions (R31) and (R36) are also exothermic, leading to a steep temperature increase and allowing the activation of reactions with higher activation energies, like the silane decomposition.

The activation of the silane decomposition reaction is the origin of an alternative reaction pathway, that is, $SiH_4 \rightarrow SiH_2 \rightarrow HSiO$, which predominates at temperatures higher than 1500 K. The overall silane consumption rate has then two peaks, one being located at about 1000 K and other at about 2000 K, and the fuel remaining from the low-temperature region is completely exhausted at the second pathway. The initiation reaction of the high-temperature route,

$$SiH_4 \rightarrow SiH_2 + H_2, \qquad (R22)$$

is a spontaneous unimolecular dissociation which, however, cannot occur at low temperatures because of its large activation temperature (see Table 1) and endothermic character, as shown by Fig. 5. This is actually the only route for the production of SiH_2 though the assumed reaction scheme gives another possible step for the production of SiH_2 (R28). The formed SiH_2 is

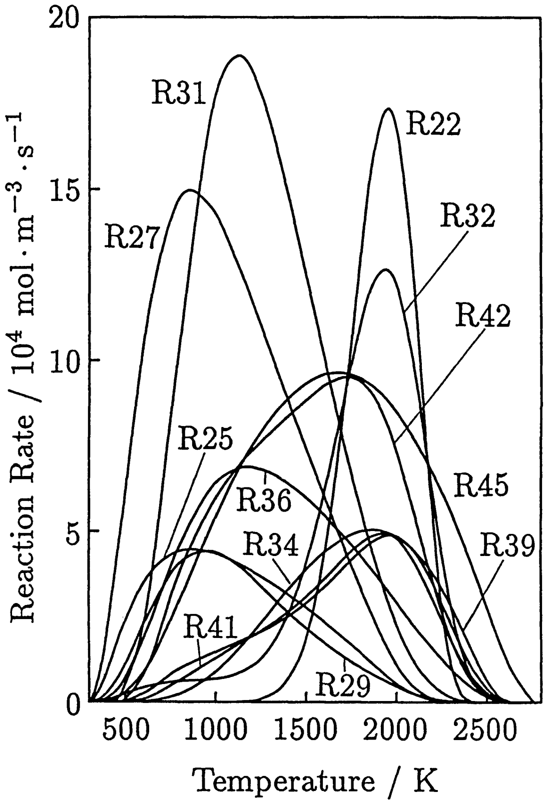

Fig. 4. Reaction rates in the stoichiometric silane flame as functions of temperature. The numbers in the figure correspond to those in Table 1.

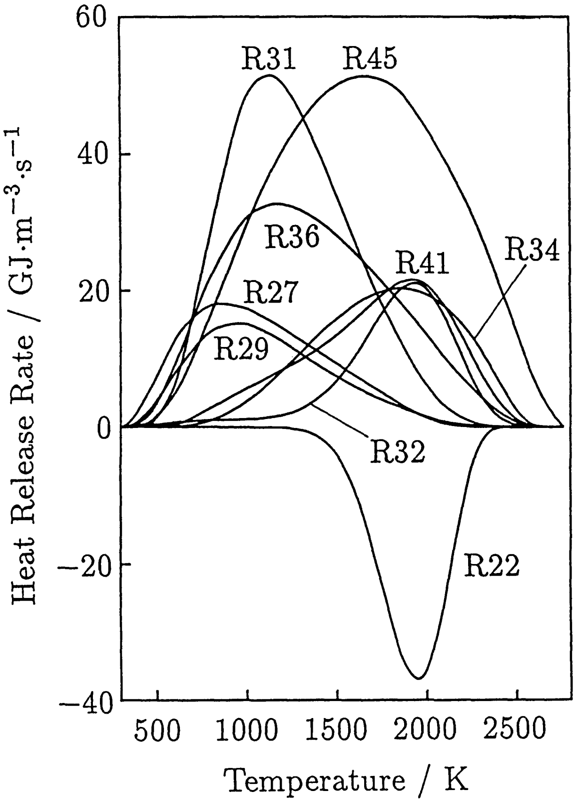

Fig. 5. Rates of heat release due to reactions in the stoichiometric silane flame.

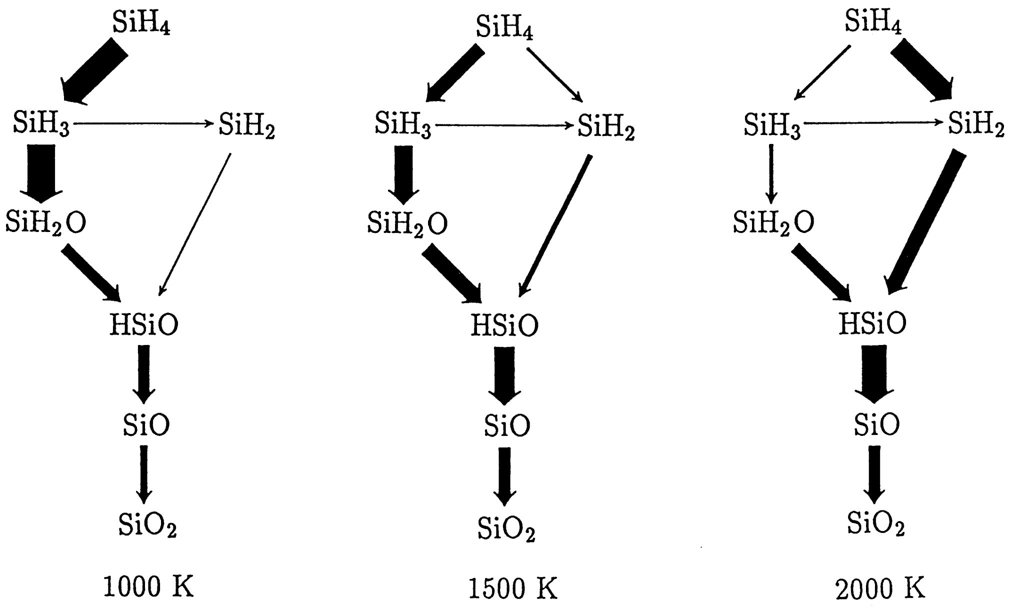

Fig. 6. Predominant reaction pathways in the stoichiometric silane flame at three temperatures. The widths of the arrows are proportional to the rates of the corresponding routes.

immediately oxidized by reaction

$$SiH_2 + O_2 \rightarrow HSiO + OH \quad \text{(R32)}$$

so that this species is not considerably accumulated in the system.

The final product SiO_2 is produced by two reactions:

$$HSiO + O_2 \rightarrow SiO + HO_2 \quad \text{(R42)}$$

and

$$SiO + O_2 \rightarrow SiO_2 + O. \quad \text{(R45)}$$

Both reactions, corresponding to the last steps of the oxidation, are activated through a wide range of temperature and constitute direct oxidation with oxygen; therefore an insufficient amount of oxygen would hinder the progression of these steps. Above 1000 K, two additional reactions,

$$HSiO + H \rightarrow SiO + H_2 \quad \text{(R39)}$$

and

$$HSiO + OH \rightarrow SiO + H_2O, \quad \text{(R41)}$$

contribute to the consumption of HSiO so that HSiO does not remain in appreciable amounts, as shown in Fig. 2.

Although the reaction scheme gives many possible ways for the silane dehydrogenation, only the reactions (R27) and (R22) are promoted around 1000 K and 2000 K, respectively. Thus, the silane consumption clearly occurs by two alternative routes, each one being well identified by the temperature activation and the intermediate species. Figure 6 illustrates the obtained reaction pathways at three temperatures in the stoichiometric silane-air flame.

Since hydroxyl radicals contribute to a great extent to the initial step of the low-temperature mechanism of silane combustion, the chemical behavior of the species which contain hydrogen and/or oxygen will be discussed. Change in a species concentration is deter-

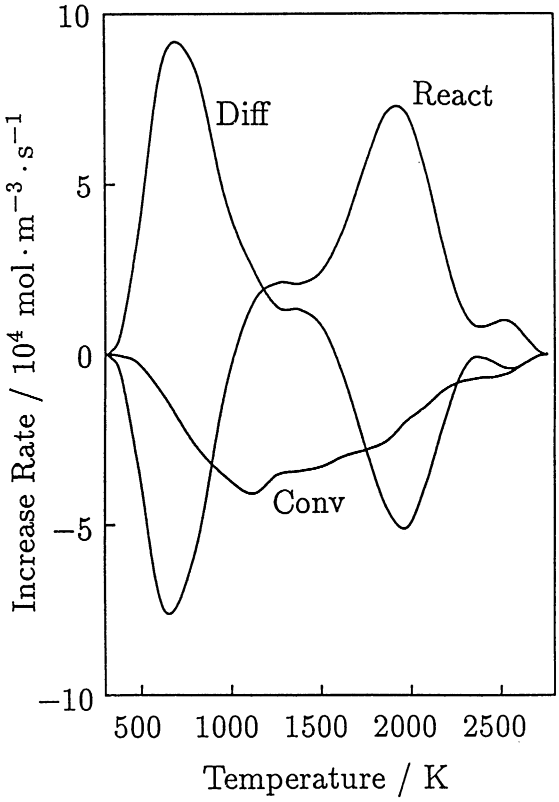

Fig. 7. Increase rates of hydroxyl radicals due to reactions (React), diffusion (Diff), and convection (Conv).

mined according to the governing equation for each species, Eq. 3. Figure 7 shows the rates of the individual terms constituting Eq. 3 for hydroxyl radicals. The reaction term expresses the net rate for the elementary reactions in which that species participates. According to the figure, hydroxyl radicals are supplied by diffusion to the low-temperature region and decrease mostly by reactions; reaction (R27) keeps the largest contribution to their consumption.

On the other hand, the reactions

$$H+O_2+M \rightarrow HO_2+M \qquad \text{(R10)}$$

and

$$H+HO_2 \rightarrow OH+OH \qquad \text{(R12)}$$

proceed with fairly large rates among hydrogen–oxygen reactions, particularly at low temperatures, though their rates are only about 1/5 of that of reaction (R27), for instance. Hydroxyl radicals are thus produced via hydroperoxyl radicals by this pair of reactions, which start from diffused hydrogen atoms supplied with a rate similar to the diffusion rate of hydroxyl radicals. Hydroperoxyl radicals, which have an interesting profile at low temperatures as shown in Fig. 3, are produced by reaction (R10) and then consumed by reaction (R12), and above 800 K are also produced by reaction (R42).

The starting point of the hydrogen–oxygen reactions in this flame is the liberation of hydrogen by reaction (R22) at high temperatures. The hydrogen is transformed into hydroxyl radicals and hydrogen atoms by the chain-branching reaction (R3) at temperatures around 2000 K, and then is oxidized by reaction (R5) also producing hydrogen atoms. The hydrogen atoms are oxidized into hydroxyl radicals by reaction (R12) reacting with the hydroperoxyl radicals. These hydroxyl radicals and hydrogen atoms are carried toward the low-temperature region by diffusion and used as the reactant of the initiation reaction (R27). Water, on the other hand, is produced in a large amount by reaction (R5) and also by the dehydrogenation reactions of the silicon-containing species with hydroxyl radicals over a wide range of temperature so that it exists widely in the flame, as shown in Fig. 1.

Rich and Lean Flames. We simulated also rich and lean silane premixed flames with equivalence ratios (ϕ) equal to 2.0, 1.43, and 0.5 to discuss the reaction mechanisms under various conditions. The calculated burning velocities are 1.8 m s^{-1} for the flame with ϕ=2.0, 2.2 m s^{-1} for ϕ=1.43, 2.2 m s^{-1} for ϕ=1.0, and 0.9 m s^{-1} for ϕ=0.5. The least square method approximating them with a cubic function of the silane content gives the maximum burning velocity of 2.6 m s^{-1} at 11%, which corresponds to an equivalence ratio of 1.2. The adiabatic flame temperature changes similarly to the burning velocity.

The oxidation of Si and H takes place in parallel in silane flames; therefore it is important to determine which oxidation takes precedence particularly under the conditions of insufficient oxygen.

Concentration profiles of silicon-containing species indicated clearly that SiH_2 remains in rich flames, and at the richest investigated condition SiH_2 increases monotonically up to 2.8% in mole fraction showing no overshoot; this species holds 19% of the silicon atoms at the final state. The rest of them are shared by SiO (59%) and SiO_2 (22%). Hydrogen atoms, on the contrary, are shared by H_2O (50%), H_2 (41%), and SiH_2 (9%). At the final state of the flame with ϕ=1.43, unburned SiH_2 still remains in a small amount, and 62% and 60% of the silicon and hydrogen atoms are kept in SiO_2 and H_2O, respectively. In the stoichiometric flame, all the silicon atoms are contained in silicon dioxide and water shares 82% of the hydrogen atoms at the final state.

Water is produced already at very early stages of combustion by reactions such as (R27) and (R31) throughout the four flames so that the oxidation of H proceeds fast at first. In the highest temperature region of the rich and stoichiometric flames, however, the produced water is reduced by the reverse reactions of (R5) and

$$OH+OH \rightarrow O+H_2O, \qquad \text{(R4)}$$

and the formed hydroxyl radicals are used by the final oxidation toward SiO_2

$$SiO+OH \rightarrow SiO_2+H. \qquad \text{(R44)}$$

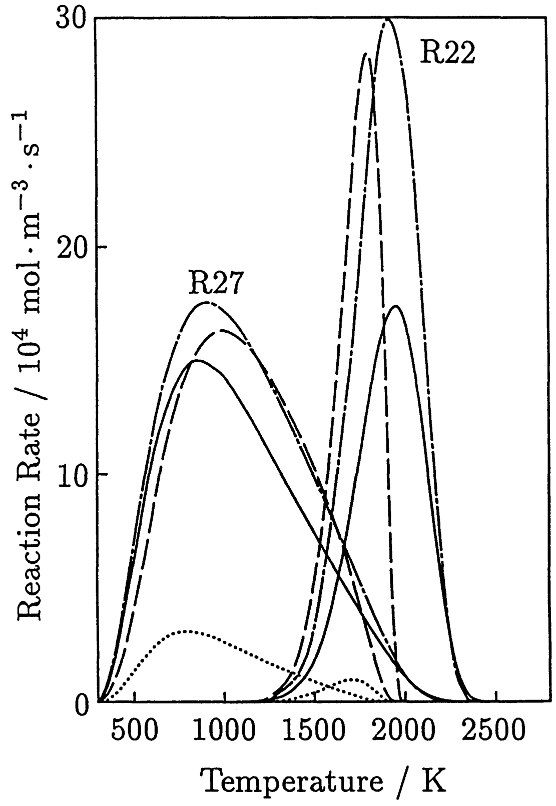

Fig. 8. Rates of reactions (R27) and (R22) in four silane premixed flames with equivalence ratio of 2.0 (dashed lines), 1.43 (dashed-dotted lines), 1.0 (solid lines), and 0.5 (dotted lines).

Formation of SiO_2 through free oxygen (reaction (R45)) is also promoted in this stage.

The rich and stoichiometric flames possess a similar low-temperature reaction mechanism, indicating that the product between the concentrations of silane and hydroxyl radicals, which determine the rate of the initiation reaction of this mechanism (R27), are almost equal one another: the maximum rates of reaction (R27) are 1.63×10^5 mol m^{-3} s^{-1} in the flame with $\phi=2.0$ (at 1000 K), 1.77×10^5 mol m^{-3} s^{-1} at $\phi=1.43$ (at 930 K) and 1.51×10^5 mol m^{-3} s^{-1} at $\phi=1.0$ (at 870 K); and those of reaction (R31) are 1.89×10^5 mol m^{-3} s^{-1} at $\phi=2.0$ (at 1210 K), 2.15×10^5 mol m^{-3} s^{-1} at $\phi=1.43$ (at 1190 K) and 1.89×10^5 mol m^{-3} s^{-1} at $\phi=1.0$ (at 1130 K). In the leanest flame, both rates are only about 1/5 of those in the above flame because of insufficient amounts of silane and hydroxyl radicals.

As for the high-temperature mechanism, on the contrary, the rates of reaction (R22) are remarkably different since this is a unimolecular reaction and its rate is simply proportional to the concentration of silane. Its maximum rate, however, becomes the largest at $\phi=1.43$ but not at $\phi=2.0$. The reason is that the flame temperature of the latter flame is much lower than that of the former one.

The rates of reactions (R27) and (R22) are consequently a good index for the reaction mechanisms in silane flames as shown in Fig. 8.

Conclusions

The simulation of silane–air flat premixed flames using a detailed reaction scheme and the analyses of the obtained results led to the following conclusions:

(I) In the flames with equivalence ratio around 1.0 the combustion reactions take place very intensely, and consequently are confined within thin areas of about 0.05 mm thick. The burning velocity of the stoichiometric flame is 2.2 m s^{-1}, Which is a little smaller than that of the hydrogen flame.

(2) Two mechanisms are provided for the reaction from SiH_4 to HSiO: one proceeds along $SiH_4 \rightarrow SiH_3 \rightarrow SiH_2O \rightarrow HSiO$ and the other along $SiH_4 \rightarrow SiH_2 \rightarrow HSiO$. These pathways are activated in different temperature ranges. The former starts even at low temperatures because it progresses as chain reactions having hydroxyl radicals as chain carriers, which are produced in a large amount even at low temperatures. The latter is activated at high temperatures because the initiation reaction of this route has a large activation temperature. The second mechanism is also accelerated under rich conditions since it starts with dissociation of silane.

References

1) C. J. Jachimowski and A. G. McLain, *NASA Tech. Rep.*, **1983**, 2129.

2) A. G. McLain, C. J. Jachimowski, and R. C. Rogers, *NASA Tech. Rep.*, **1985**, 2415.

3) S. Koda, O. Fujiwara, and T. Ohnishi, *Combust. Flame,* **65**, 121 (1986).

4) S. Koda and O. Fujiwara, "Twenty-first Symposium (International) on Combustion," The Combustion Institute, Pittsburgh (1986), p. 1861.

5) S. Koda and O. Fujiwara, *Combust. Flame,* **73**, 187 (1988).

6) S. Suga and S. Koda, *Jpn. J. Appl. Phys.*, **27**, L1966 (1988).

7) S. Koda and O. Fujiwara, "ISPC-8 Tokyo," Tokyo (1987), p. 2022.

8) K. Tokuhashi, S. Horiguchi, Y. Urano, M. Iwasaki, H. Ohtani, and S. Kondo, *Combust. Flame,* **82**, 40 (1990).

9) J. R. Hartman, J. Famil-Ghiriha, H. A. Ring, and H. E. O'Neal, *Combust. Flame,* **68**, 43 (1987).

10) S. Fukutani, N. Kunioshi, and H. Jinno, *Bull. Chem. Soc. Jpn.,* **63**, 2191 (1990).

11) S. V. Patankar, "Numerical Heat Transfer and Fluid Flow," Hemisphere Publishing Co., New York (1980), Chap. 3.

12) D. L. Baulch, D. D. Drysdale, D. G. Horne, and A. C. Lloyd, "Evaluated Kinetic Data for High Temperature Reactions," Butterworths, London (1972), Vol. 1.

13) J. Warnatz, "Combustion Chemistry," ed by W. C. Gardiner, Jr., Springer-Verlag, New York (1984), pp. 197—360.

14) D. E. Jensen and G. A. Jones, *Combust. Flame,* **32**, 1 (1978).